Shaping Kale Morphology and Physiology Using Precision LED Light Recipes

Sabine Scandola[1,2,*], Lauren E. Grubb[1,*], Brigo Castillo[1], Lexyn Iliscupidez[1], Curtis Kennedy[1,3], Nicholas Boyce[1], Mohana Talasila[1], and R. Glen Uhrig[1, 4,#]

[1] Department of Biological Sciences, University of Alberta, Edmonton, Alberta, Canada

[2] Lethbridge Research and Development Centre, Agriculture and Agri-Food Canada, Lethbridge, Canada

[3] Department of Computer Science, University of Alberta, Edmonton, Alberta, Canada

[4] Department of Biochemistry, University of Alberta, Edmonton, Alberta, Canada

[*]These authors contributed equally (S.S. and L.E.G.)

[#] Senior and corresponding author:

Dr. R. Glen Uhrig
Department of Biological Sciences,
University of Alberta,
Edmonton, Alberta, Canada, T6G 2E9
Email: ruhrig@ualberta.ca
Phone: +1 780 492 3088
Fax : +1 780 492-9234ruhrig@ualberta.ca

Running Title: Light condition effects on kale growth and development

Key Words: Kale, Anthocyanins, Light emitting diodes (LEDs), Horticulture, PhotosynQ, Quantitative Proteomics, Metabolomics

Abstract

Light emitting diodes (LEDs) present an innovative opportunity for manipulating plant growth and development. Light serves as a fundamental energy source and an environmental cue, providing an ability to control plant traits through the precise manipulation of light intensity and quality. Here, we assess effects of light intensity and spectral composition on the growth and physiology of the important model plant: Kale (*Brassica oleracea*), known for its phenotypic plasticity and nutritional composition, kale is a crop well-suited for indoor cultivation. Here, we employ a combination of advanced phenotyping, computer vision, gas chromatography-mass spectrometry (GC-MS) metabolomics, and liquid chromatography-mass spectrometry (LC-MS)-based quantitative proteomics to characterize the molecular changes that underpin light-dictated differences in the growth and metabolism of two different kale cultivars under different light intensity and spectral composition scenarios. We identify time-of-day and cultivar-specific light intensity and spectral composition-induced changes related to growth, shade avoidance, photosynthesis and several nutritional components including amino acids, glucosinolates and carotenoids. Our results offer a key resource to the plant community and demonstrate the translational potential of light manipulation in tailoring kale growth and nutritional content for enhanced crop productivity and/or health benefits, while simultaneously offering a more cost-effective solution for contemporary agricultural challenges.

1 Introduction

Kale (*Brassica oleracea*), also known as leaf cabbage, belongs to the large *Brassicaceae* family that includes cauliflower, broccoli and collard greens. Established as a superfood, this leafy green is rich in fiber and essential vitamins, as well as antioxidants such as flavonoids, each of which have been shown to positively affect cardiovascular and gastrointestinal health[1]. To date, the health benefits of kale have been heavily studied, with researchers continuing to identify new anti-cancer (e.g. sinigrin, spirostanol)[2] and neuroprotective (e.g. sulforaphane)[3] compounds, which neutralize reactive oxygen species. Further, kale demonstrates excellent temperature resilience resulting from its waxy coating and high production of polyamines[4], rendering it a valuable agricultural crop in the context of climate change[5].

Kale is also well-suited for indoor growing facilities. As a leafy green, it is a favored choice for horticultural growers as it has a quick harvest cycle with minimal space and resource requirements[6], appealing to both growers as well as consumers looking for fresh, locally-sourced produce[7]. Indoor / vertical farms have strongly co-evolved with new technologies as the promise of providing fresh and locally grown food largely relies on reducing production costs through technological advancements[8]. In this context, LED technology has revolutionized indoor farming, providing a wide range of energy-efficient and versatile lighting options. For example, unlike traditional light sources (e.g. incandescent bulbs, fluorescent tubes, metal halide or high pressure sodium bulbs), LED lighting systems offer an ability to fine-tune the spectral composition and intensity of the applied light[9]. Light is critical for photosynthesis, which drives plant metabolism[10], while plant photoreceptors, such as phytochromes and cryptochromes, respond to light quality, impacting processes such as plant growth (e.g. biomass) and development (e.g. flowering)[11]. However, despite our understanding of kale at a phenotypic level, we lack knowledge of how light impacts kale at the molecular level, limiting our ability to enhance genetics through targeted breeding or biotechnology approaches.

To date, elementary changes in spectral composition have been shown to affect kale phenotypic and metabolic profiles[12]. Blue light enhances growth and nutritional qualities[13], while red light affects kale pre- and post-harvest by altering nutrient and chlorophyll content[14]. Similar to red light, far-red light enhances photosynthetic rates through the Emerson effect[15]. Beyond specific light types, light wavelength ratios also play an essential role in how phytochromes

perceive and transduce light signals[16], offering opportunities to build precise light recipes that maximize traits of interest.

To better exploit currently available kale genetics, we endeavored to precisely resolve the impacts of light intensity and spectral composition on kale growth, development and nutritional content by contrasting the diel molecular changes in two related kale cultivars: Dwarf curled scotch (K3) and Red Scarlet (K9). While there are many kale cultivars, each with unique morphologies, growth parameters and nutritional characteristics[17], our previous study examining nine commercially available kale cultivars found that K3 and K9, both *Brassica oleracea var. sabellica*, showed the most diversity in their phenotypes and molecular characteristics[17], allowing us here to capture an in-depth understanding of how light properties impact kale growth and development in order to establish a compendium of molecular changes that can be utilized by the broader community. We specifically took a diel experimental approach to analyzing the effects of light intensity and spectral composition by harvesting tissues at end-of-day (ED, ZT11 (zeitgeber)) and end-of-night (EN, ZT23) time-points as both the proteome and metabolome are known to undergo substantial diel changes[17]. Understanding how external factors such as time-of-day intersect with differences in light intensity and quality to impact kale physiology is essential for determining optimal horticultural growing conditions and harvesting times to extract maximize value, as well as inform future efforts in breeding more productive and nutritious kale varieties.

2 Materials and Methods

2.1 Plant material and cultivation

Dwarf Curled Scotch (K3) and Red Scarlet (K9) kale seeds (*B. oleracea var. sabellica*) were purchased from West Coast Seeds (https://www.westcoastseeds.com/). Seeds were surface sterilized with incubations in 70% (v/v) ethanol and 30% (v/v) bleach solutions at room temperature beginning with a 4-minute incubation in 3 mL of 70% (v/v) ethanol. The seeds were then rinsed with 3 mL of sterile milli-Q water and 3 mL of 30% (v/v) bleach was added onto each tube for a 7-minute incubation with periodical shaking every 2 minutes. Finally, the bleach solution was decanted, and the seeds were rinsed three times with 3 mL of sterile Milli-Q water. Following sterilization, seeds from each cultivar were plated onto 0.5 x Murashige and Skoog (MS) media plates containing 1% (w/v) sucrose. The seeds were then stratified at 4 °C in total darkness for 4 days. Following stratification, the kale seedlings were entrained to their

respective light treatment for 7 days. To prepare the soil for seedling transplant, ~25 kg of soil (Sun Gro Sunshine Mix #1) was mixed with 8 L of H_2O and then transferred onto 4" square polypropylene pots. Transplantation occurred once most plants had reached the cotyledon stage at 11 days post-imbibition (dpi).

2.2 Light Conditions

The programmable LED (Perihelion Model) lights used for this experiment were provided by G2V Optics Inc. and were installed inside ventilated growth chambers lined with reflective mylar. The kale plants were grown under a 12-hour light and 12-hour dark regiment. Three different light intensities were tested: 75, 125, 175 PPFD ($\mu mol.m^{-2}.s^{-1}$) (**Supp Figure 1A**). Spectral light conditions were assigned in spectral ratios of R/B and R/FR of low R/B or R/FR, balanced light and high R/B or R/FR (**Supp Figure 1B**).

2.3 Measurement of Kale Photosynthetic Performance via MultisynQ

Photosynthetic performance was measured following the Photosynthesis RIDES 2.0 protocol using a MultispeQ v1.0 (PhotosynQ LLC, USA)[18]. At mid-day (zeitgeber; ZT6) 34 dpi, the photosynthetic performance of the kale plants was measured by clamping the second true leaf between the MultisynQ sensors ensuring full coverage. The leaf remained in the chamber until the data collection process was completed (~10 s). A total of 10 randomly selected plants were analyzed for each cultivar and light condition.

2.4 Phenotyping measurements

Plants were grown in separate chambers under different light intensity and spectral conditions (**Supp Figure 1**). Each chamber was equipped with single-board Raspberry Pi 3 B+ computers and ArduCam Noir Cameras (OV5647 1080p) with a motorized IR-CUT filter and two infrared LEDs. Pictures of plants were taken every 5 minutes. Plant surface area analysis across light conditions was performed by averaging the area of each plant measured during a 1-hour period (between ZT6 and ZT7) at 22 dpi. Plant surface areas were extracted using Python scripts from the open-source software package PlantCV (https://plantcv.readthedocs.io/), following the methodology previously described[19].

2.5 Harvesting and Sample Processing

At 35 dpi, kale leaves were harvested at two time points: end-of-night (ZT23) and end-of-day (ZT11). This was done to capture the expansive metabolic changes occurring during the transitions between night-to-day and day-to-night, respectively. Leaves from three kale plants of

the same cultivar were pooled into a labelled 50 mL conical tube and promptly frozen in liquid nitrogen to preserve the proteins and metabolites present. In total, four tubes were collected from each cultivar per chamber during harvest. Two metal beads were then introduced into each conical tube and the samples were ground by subjecting them to 3x – 30 s/1200 rpm using a Geno/Grinder® - Automated Tissue Homogenizer and Cell Lyser. 100 mg (±1 mg) of each finely-ground sample was then portioned into each of two separate 2 mL Eppendorf Safe-Lock tubes for further processing.

2.6 Anthocyanin Extraction and Quantification:

Anthocyanin analysis was performed as previously described by Neff and Chory (1998), with the following modifications. Specifically, 500 µL of 100% (v/v) methanol-1% (v/v) hydrochloric acid was added to each tube containing the finely ground samples and incubated at 4 °C for 24 hours in darkness. From there, 200 µL of H_2O and 500 µL of chloroform were added and the tubes were centrifuged at 18,000 x g for 5 minutes at room temperature. 400 µL of the supernatant was then transferred over to new tubes and adjusted to a total volume of 800 µL with 60% (v/v) methanol-1% (v/v) hydrochloric acid. A total of 200 µL from each volume-corrected sample was transferred into a well in a 96-well plate and absorbance at 530 nm and 657 nm was measured with a Tecan Spark® plate reader using 60% (v/v) methanol -1% (v/v) hydrochloric acid as the background. The relative anthocyanin content was then derived mathematically using: $Antho = (Abs_{530} - Abs_{657}) \times 1000 \times powder\ weight\ (mg)^{-1}$.

2.7 Metabolite analysis via Gas Chromatography Mass Spectrometry (GCMS)

2.7.1 Metabolite extraction: A total of 700 µL of ice-cold 100% (v/v) methanol was added to the tubes containing 100 mg of finely ground leaf sample and promptly vortexed for ~20 seconds. Using a thermomixer, these were then incubated for 15 minutes at 70 °C with shaking at 1200 rpm. From there, the tubes were centrifuged at 18,000 rpm for 15 minutes and the supernatants were transferred into new tubes. The pellet was then re-extracted using 700 µL of 50% (v/v) methanol containing Ribitol at 25 µL per sample at 0.4 mg/mL in water and vortexed for ~20 seconds until re-suspended. These tubes were then centrifuged at 14,000 rpm for 10 minutes and 600 µL of the supernatant was combined with the previous supernatant. Finally, 100 µL was transferred into new tubes and dried using a vacuum centrifuge at 1 torr at room temperature for 1.5 - 2 hours.

2.7.2 Gas chromatography mass spectrometry analysis:

The dried samples were derivatized by adding 100 µL of methoxamine hydrochloride into each tube and then incubated at 30 °C at 850 rpm for 1 hour using a Thermomixer F2.0 (Eppendorf). Subsequently, 50 µL of N,O-bis(trimethylsilyl)trifluoroacetamide (BSTFA) was added to each tube and incubated at 50 °C at 850 rpm for 3 hours using a Thermomixer F2.0 (Eppendorf). A total of 150 µL of each sample was then transferred to vials in preparation for injection in the GC-MS. Samples were analyzed via a 7890A gas chromatograph (Agilent) paired to a 5975C quadrupole mass detector (Aglient). The initial GC oven temperature was set at 70 °C and then increased to 325 °C at 7 °C per minute two minutes post-injection where the temperature was then maintained at 325 °C for 3.6 minutes. The injection and ion source temperatures were set to 300 °C and 230 °C, respectively with a solvent delay of 5 minutes. The helium flow rate was also adjusted to a rate of 1 mL/minute. Measurements were performed with electron impact ionization (70 eV) in full scan mode (m/z 33-600). Identification of metabolites was performed based on their mass spectral and retention time index, and how closely they matched to those acquired from the National Institute of Standards and Technology library and the Golm Metabolome Database.

2.8 *Protein extraction and LC-MS analysis*

2.8.1 Protein extraction and LC-MS data acquisition

Kale leaf tissue harvested at ZT23 and ZT11 was flash-frozen in liquid N_2. Tissue was ground in liquid N_2 using a mortar and pestle and aliquoted into 400 mg samples (n=4 replicates). Samples were extracted with 50 mM HEPES-KOH pH 8.0, 50 mM NaCl, and 4% (w/v) SDS at a ratio of 1:2 (w/v). Next, samples were vortexed followed by incubation for 15 min at 95 °C using a Thermomixer F2.0 (Eppendorf) shaking at 1,100 rpm. Samples were subsequently incubated at room temperature for an additional 15 min of shaking followed by clarification at 20,000 x g for 5 min at room temperature, where the supernatant was then retained in fresh Eppendorf microtubes. Protein concentration was estimated by bicinchoninic (BCA) assay (23225; Thermo Scientific), followed by sample reduction using 10 mM dithiothreitol (DTT) for 5 min at 95 °C. Following cooling to room temperature, samples were alkylated using 30 mM iodoacetamide (IA) in dark for 30 min at room temperature without shaking. The alkylation was stopped by addition of 10 mM DTT, followed by a brief vortex and 10 min room temperature incubation without shaking. Samples were digested overnight with 1:100 sequencing grade trypsin (V5113; Promega), followed by quantification of the generated peptide pools using a Nanodrop (Thermo Scientific). Subsequently, samples were acidified with formic acid to a final concentration of 5% (v/v) followed by drying by vacuum centrifugation. Peptide desalting was then performed using

ZipTip C18 pipette tips (ZTC18S960; Millipore), with peptides subsequently dried and dissolved in 3% (v/v) ACN / 0.1% (v/v) FA prior to MS analysis. A Fusion Lumos Tribrid Orbitrap mass spectrometer (Thermo Scientific) was used to analyse the digested peptides in data independent acquisition (DIA) mode using the BoxCarDIA method as previously described[20]. 1 µg of dissolved peptide was injected using an Easy-nLC 1200 system (LC140; ThermoScientific) and a 50 cm Easy-Spray PepMap C18 column (ES903; ThermoScientific). Liquid chromatography and BoxCarDIA acquisition was performed as previously described[20].

2.8.2 Proteomic Data Analysis

All acquired BoxCarDIA data was analyzed using a library-free approach in Spectronaut v14 (Biognosys AG) under default settings. The *B. oleracea* var. *oleracea* proteome (Uniprot:https://www.uniprot.org/ containing 58,545 proteins) was used for data searching. Default search parameters were used for proteome quantification including: a protein, peptide and PSM FDR of 1%, trypsin digestion with 1 missed cleavage, fixed modification including carbamidomethylation of cysteine residues and variable modification including methionine oxidation. Data was Log2 transformed and median normalized with significantly changing differentially abundant proteins determined and corrected for multiple comparisons (Bonferroni-corrected p-value <0.05; q-value).

2.9 *Bioinformatics*

Gene Ontology (GO) enrichment analysis was performed using the Database for Annotation, Visualization and Integrated Discovery (DAVID; v 6.8; https://david.ncifcrf.gov/home.jsp).A) using a significance threshold of p-value < 0.01. Conversion of *B. oleracea* gene identifiers to Arabidopsis was performed using Uniprot (https://www.uniprot.org/) followed by Ensembl Biomart (https://plants.ensembl.org/biomart) for STRING association network analysis and metabolic pathway analysis. STRING association network analysis was performed using Cytoscape v3.10.1 (https://cytoscape.org) in combination with the String DB plugin stringApp and an edge threshold of 0.95. Visualization of GO dotplot was performed using R version 4.3.1 and *ggplot2* package. Metabolic pathway enrichment was performed using the Plant Metabolic Network (PMN; https://plantcyc.org) with enrichment determined using a Fisher's exact test (p-value < 0.01). Final figures were assembled using Affinity Designer (v.2.4.1).

3 Results and Discussion

3.1 Light intensity and spectral composition influence kale morphology

We first investigated the effects of light intensity and spectral composition on the morphology of kale. For our light intensity experiments, plants were grown under three different light intensities: 75, 125 and 175 PPFD (**Supp Figure 1A**). We found a relatively linear relationship between light intensity with plant fresh weight and surface area in both cultivars at 35 dpi (**Figure 1A-B**). Consistent with our observations, previous studies have reported a linear relationship between light intensity and fresh weight in pea microgreens[21], as well as kale, cabbage, arugula and mustard[22]. Importantly, these studies used PPFD up to 600 $\mu mol \cdot m^{-2} \cdot s^{-1}$, with increases in fresh weight even at the upper PPFD values, suggesting our highest light intensity of 175 PPFD does not invoke a high light-induced stress response. As light intensities used in vertical farming are typically lower, around 200 PPFD[23–25], our study is highly relevant for informing practices of kale grown in indoor farms, in addition to examining the feasibility of growing kale on a smaller, more economical scale for home growers or with lower energy usage / footprint. We next examined the effect of light intensity on diel leaf anthocyanin content, which provides plant coloration to attract pollinators, but also acts as an antioxidant with benefits to human health[26]. Although anthocyanins could not be detected in K3, the K9 cultivar, which is known to produce anthocyanins, typically showing red colouration, did not show a significant difference in anthocyanin concentration with increasing light intensity (**Figure 1D**). Anthocyanins are typically produced in response to stressful conditions[27], thus it is possible that our use of a lower light intensity than that experienced outdoors, combined with the stage of growth, resulted in lower anthocyanin content.

Our spectral composition experiments consisted of modulating the ratio of red to blue (R/B) and red to far-red (R/FR) light, while maintaining an otherwise balanced spectra and a light intensity of 125 PPFD (**Supp Figure 1B**). Previous studies have shown a high R/B ratio promotes plant growth[28], whereas a low R/B ratio promotes accumulation of beneficial anthocyanins[29]. In our experiments, K3 exhibited an increase in fresh weight with increasing R/B with no corresponding change in surface area, whereas K9 showed no change in fresh weight, but an increase in plant surface area with increasing R/B and R/FR (**Figure 2A-B**), indicating that red light may be particularly important for K9 growth. Supporting this possibility are observed increases in dry mass and seedling area specifically in red kale varieties under elevated red light, whereas blue light had a stronger effect on green kale dry mass[30], suggesting spectral composition impacts on growth are cultivar specific. This emphasizes the need to generate cultivar-specific molecular response data, such as that generated here, to uncover unique breeding opportunities and inform growers choosing genetics for indoor farming. We additionally observed changes in K9 anthocyanin content with modulated spectral composition

(**Figure 2C**). Consistent with previous reports, an increase in R/B induced a decrease in anthocyanin content, whereas an increase in R/FR stimulated anthocyanin production at both timepoints (**Figure 2C**). Therefore, our results show that changing light intensity and spectral composition impacts kale morphological characteristics and anthocyanin levels.

3.2 Modulating light intensity and spectral composition impacts kale photosynthetic performance

We next measured light intensity- and spectra- induced changes in a suite of photosynthetic parameters alongside relative chlorophyll levels using a MultispeQ device[18] (detailed in **Table 1; Supp Figure 2**). In particular, ΦPSII, which represents how much light energy is absorbed by photosystem II[18], and chlorophyll content (SPAD), were both impacted by changes in light intensity and spectral composition. Increases in light intensity (**Figure 1C**) and R/FR (**Figure 2C**) resulted in increasing SPAD in both cultivars, whereas increasing R/B resulted in a SPAD decrease (**Figure 2C**). Similarly, ΦPSII increased under increasing light intensity, but in the K9 cultivar only (**Figure 1C**), while an increase in ΦPSII was found in both cultivars with increasing R/FR (**Figure 2C**). Conversely, an increasing R/B ratio resulted in a decrease in ΦPSII (**Figure 2C**). Our finding of increased ΦPSII with increasing light intensity aligns with previous observations in lettuce where the highest ΦPSII was found at 200 PPFD across a range of 100 to 800 PPFD, which is comparable to our 175 PPFD treatment[31]. Furthermore, blue light is found to be more important than red light in modulating photosystem I and II activity and photosynthetic electron transport capacity in cucumber[32], consistent with our increasing R/B ratio showing lower SPAD and ΦPSII. Overall, our results indicate that kale photosynthetic parameters and chlorophyll content can be modulated by changes in light intensity and spectral composition.

3.3 Analysis of total proteome changes with altered light intensity and spectral composition

To contextualize the observed phenotypic changes, we used quantitative proteomics to assess the protein-level changes in both K3 and K9 over the varying light intensities and spectral compositions. This analysis quantified a total of 5,493 proteins across our intensity experiments, and 6,527 proteins across spectra experiments (**Supp Table 1**). We queried this data for significantly changing proteins by comparing each varied light intensity or spectra to the lowest treatment condition. Thus,125 PPFD and 175 PPFD were compared to 75 PPFD (**Figure 3A; Supp Table 1**) and balanced and high spectral compositions compared to low (**Figure 3B-C Supp Table 1**).

Using these significantly changing proteins, we undertook gene ontology (GO) enrichment analysis to resolve biological processes underpinning plant response to the changing light intensity and spectral composition (**Figure 3D**). Here, we find an enrichment in biological processes related to cell wall and cell cycle, response to oxidative stress and hormone signaling, along with extensive changes in multiple aspects of metabolism including: sterol biosynthesis, photosynthesis and pigment metabolism, carbohydrate metabolism, glycolysis and glucosinolate production. We next refined our GO analysis results by performing association network analysis using STRING-DB (https://string-db.org/; edge score > 0.7) to define hubs of associated proteins exhibiting cultivar or time-of-day responses. To do this, we used the significantly changing proteins induced by a change in light intensity (**Figure 4**), R/B (**Figure 5A**) and R/FR (**Figure 5B**). As the closely related kale relative, *Arabidopsis thaliana* (Arabidopsis), has more extensive bioinformatic resources, we first converted the *B. oleracea* gene identifiers for all quantified proteins in the study to Arabidopsis gene identifiers (AGI) using a combination of UniProt (https://www.uniprot.org/) and Ensembl Biomart (https://plants.ensembl.org/biomart). This identified unique AGIs for 90% of the significantly changing proteins in our intensity experiments (2395/2662), along with 88.9% (2222/2499) and 89.4% (2520/2819) of proteins in our R/B and R/FR spectra experiments; respectively. Along with validating enriched biological processes, the association network also indicated changes in amino acid metabolism, phenylpropanoid metabolism, proteolysis and RNA splicing.

Interestingly, several of the enriched biological processes could be attributed to the plant shade avoidance response, or relief thereof, including the changes in hormone signaling such as brassinosteroid (BR) and auxin signaling, cell wall organization / biogenesis and photosynthesis. Plant shade avoidance response is associated with conditions that mimic shading, including low light intensity, low blue light and low R/FR ratios[33] and has been linked to increased BR[34–36] and auxin signaling[37]; both of particular importance for shade-induced hypocotyl elongation. Within our dataset, we find a down-regulation of BR signaling in K3 with increasing light intensity at ZT11, and an up-regulation of auxin-activated signaling pathway with increasing R/B at ZT11. Both observations are consistent with a relief of shade avoidance responses with our increasing intensity experiments, and an induction upon growth under decreased blue light.

Further, BR shade avoidance response is related to changes in cell wall structure, particularly through the action of xyloglucan endotransglucosylase/hydrolases (XTHs) and expansins (EXPAs), with cell wall modification promoting elongation of the hypocotyl to drive growth toward light[38]. Our data find a multitude of cell wall proteins changing in abundance in

response to both light intensity and spectral composition, potentially driving shade relief-like responses in both kale cultivars. We specifically note a down-regulation of cell wall organization proteins, primarily XTHs, EXPAs, and pectinesterases (PMEs) with increasing light intensity and R/FR ratio, combined with an up-regulation of XTHs with increasing R/B, which is consistent with changes in the plant perception of shade and hypocotyl elongation. Interestingly, more members of the XTH family were down-regulated in K9 with increasing light intensity and K3 with increasing R/FR, suggesting K9 may be more sensitive to changes in intensity and K3 more sensitive to changes in red light wavelengths, a finding that agrees with our growth and morphology observations.

Beyond its impact on shade avoidance, light intensity and quality critically impact plant photosynthesis and light harvesting, as well as pigment metabolism (e.g. chlorophyll and carotenoids). Intriguingly, our proteomics data reveal a concurrent down-regulation of light harvesting proteins under higher light intensity conditions at ZT23 in K3, with LHCA1 (A0A0D3CTW2; A0A0D3DT59), LHCA2 (A0A0D3DUU9; A0A0D3BWE5), LHCA3 (A0A0D3E520), LHCB2.4 (A0A0D3DBD3), LHCB4.2 (A0A0D3CLT0) and LHCB5 (A0A0D3BQY2) all down-regulated. Alternatively, we only find LHCA2 and LHCB5 were down-regulated in the K9 cultivar, indicating a stronger response in K3. This may result from sufficient, or even excessive light energy under the 175 PPFD light intensity, such that light harvesting potential has been reached, a phenomenon which is well-established in response to light/shade levels[39–41]. Correspondingly, under a higher R/FR ratio we also find the down-regulation of light harvesting proteins, consistent with relief from conditions that promote shade avoidance responses. By contrast, under a balanced ratio we see an up-regulation of light harvesting and photosynthesis-related proteins, particularly in K9 at ZT11, suggesting an optimal ratio of R/B light is best for light harvesting and photosynthetic responses in kale. This is consistent with excessive amounts of red light resulting in an imbalance in PSI and PSII, and thus blue light being required for optimal photosynthetic efficiency[42]. Overall, our data suggest light-dependent differences exist between the two cultivars, with K3 light harvesting proteins showing a stronger response to light intensity changes, and K9 more responsive to changes in spectral composition.

3.4 Analysis of metabolite changes with modified light intensity and spectral composition

With a multitude of metabolic pathways enriched in our GO and STRING-DB analyses, we next used the Arabidopsis orthologs for the significantly changing proteins with increasing intensity, R/B and R/FR to perform metabolic pathway analysis using the Plant Metabolic Network (PMN;

https://plantcyc.org; **Supp Tables 2-4**). Here, enriched metabolic pathways further corroborated our GO and STRING-DB association network analyses, resolving pathways for photosynthesis and respiration, amino acid metabolism, pigment metabolism, glycolysis, carbohydrate metabolism, oxidative stress responses, glucosinolate production and sterol biosynthesis. We next sought to determine how these changes in metabolic pathway protein abundance translate into bonified plant metabolic outcomes, using GC-MS to quantify changes in the metabolite content of each cultivar under each light conditions (**Figure 6; Supp Figure 3; Supp Table 5**), R/B ratio (**Figure 7; Supp Figure 4-6**). Amino acids (16), fatty acids (3), organic acids (11), polyamines (2), sterols (2), sugars (5), and sugar alcohols (2) were detected and quantified.

Amino acids - Our proteome analysis indicated changes in amino acid metabolism for both cultivars in response to changing light intensity and spectral composition (**Supp Figure 6**). Our metabolite analysis found extensive changes in the glutamate-derived family of amino acids, which includes glutamic acid, glutamine, GABA, proline and arginine. These amino acids typically account for the highest amino acid proportions in plants, with glutamic acid and proline present at the highest quantity in kale[43]. Glutamate metabolism also represents a critical link between nitrogen and carbon metabolism through the TCA cycle, with several products of glutamate catabolism, including proline and GABA, associated with plant stress response[44,45].

In both cultivars, we observed a general increase in glutamic acid and proline at both time-points with increasing light intensity. GABA increased in ZT11 in both cultivars at ZT11, but at ZT23 there was a decrease in GABA in K3 and an increase in K9. Increased glutamic acid abundance with increasing light intensity coincided with our proteome-based metabolic pathway analysis, where we identified down-regulation of proteins involved in glutamate catabolism. This included GLUTAMATE DEHYDROGENASE1 (GDH1; A0A0D3EEJ0) and GDH2 (A0A0D3AI31), which convert glutamate to glutamine, DELTA-1-PYRROLINE-5-CARBOXYLATE SYNTHASE B (P5CSB; A0A0D3BXP3), involved in proline biosynthesis, N-ACETYLGLUTAMATE SYNTHASE (NAGS; A0A0D3A172) and N-ACETYLGLUTAMATE KINASE (NAGK; A0A0D3BX89), which are steps toward ornithine biosynthesis, and CARBAMOYL-PHOSPHATE SYNTHASE ALPHA (CARA; A0A0D3CZA9), which drive arginine biosynthesis. We found this trend in both K3 and K9 and at both time-points, suggesting increasing the light intensity in our experiments may relieve stress responses associated with low light. The increase in proline concentration under higher light intensities, however, may suggest sufficient levels of proline with downregulation of P5CSB to prevent further accumulation.

We find similar results in our increased R/B ratio proteome data with proteins associated with proline biosynthesis and glutamate metabolism primarily down-regulated at ZT23 in both K3 and K9. This manifested as an increase in glutamic acid in both cultivars at both time-points. Proline levels were not responsive to R/B increase, while glutamine peaked under balanced light condition at ZT11 and decreased at ZT23. Alternatively, increasing R/FR spectral composition induced the most changes in metabolite content of glutamate family amino acids. Interestingly, metabolite data indicated peak glutamic acid, glutamine and GABA levels in both K3 and K9 under balanced light conditions. This may indicate that balanced light conditions are associated with the lowest stress and most balanced C/N metabolism during the day.

The aspartate-derived amino acids are also of great importance for human nutrition as they cannot be synthesized by the human body and must be obtained through diet[46]. This includes the essential amino acids lysine, threonine, methionine and isoleucine. Of particular interest is lysine, as it is generally of very low abundance in plants[47]. Within our proteome metabolic pathway analysis, lysine biosynthesis is enriched among down-regulated proteins as light intensity increases, particularly in K3 at ZT11, with a down-regulation of ASPARTATE KINASE (AK2) and of DIHYDRODIPICOLINATE SYNTHASE1 (DHDPS1); both involved in lysine biosynthesis. However, within our metabolite data, there is a significantly higher amount of lysine present in K3 under 125 PPFD than either 75 or 175 PPFD, suggesting more complex regulation mechanisms. Regulatory complexity has previously been observed in attempts to engineer greater lysine production, where lysine has been shown to allosterically inhibit the activity of DHDPS1[48], as well as impact the abundance of other aspartate-derived amino acids, such as threonine[49]. In contrast to increasing light intensity, increasing R/B and R/FR ratios showed enriched lysine biosynthesis metabolic pathway among up-regulated proteins, suggesting a greater proportion of red light may promote lysine biosynthesis. Our metabolite data suggested that lysine levels could be modulated by changing light intensity and spectra, with a peak at 125 PPFD for both cultivars at ZT23, and a peak under balanced light in K3 at ZT23. Thus, our results suggest the difficulty in engineering lysine levels in kale may be possible by carefully modulating a combination of light intensity and spectral composition.

Finally, we noted cultivar-specific differences in glycine content with increasing intensity. We observed decreased glycine abundance with increasing light intensity in K3, but increased glycine in K9. Previously, we observed differential accumulation of glycine forming the major difference between sub-groups containing K3 and K9[17]. Although we did not observe much change in serine content, both glycine and serine are key to the functioning of primary

metabolism and photorespiration[50], and thus this difference may point to cultivar specific mediation of primary metabolism response to differing light intensity.

Carbohydrates – Our proteomic analysis revealed changes in carbohydrate metabolic proteins across each light intensity and spectral composition manipulation treatment. We also find that this manifested in the differential abundance of several sugars in our metabolite analysis, including fructose, glucose, mannose-6-phosphate (M6P) and trehalose. In our proteomic data, we observe a general down-regulation of proteins involved in glycolysis and starch degradation, as well as trehalose biosynthetic proteins with increasing light intensity. As trehalose has been associated with shade avoidance[51] and regulation of the circadian clock[52], this is consistent with reduced stress under low light intensities associated with shade as we increase the light intensity from 75 to 175 PPFD. We also find that increasing the R/B ratio down-regulates proteins associated with glycolysis in both cultivars, as well as mannose metabolism in the K9 cultivar only. This was consistent with the lowest M6P levels found in K9 under balanced light conditions. Finally, increasing R/FR was associated with the down-regulation of glycolytic proteins in both cultivars, as well as myo-inositol biosynthetic proteins in K9. Conversely, myo-inositol biosynthesis was up-regulated in K3 with increasing R/FR. In K3, this correlates with corresponding metabolite levels, as the myo-inositol level was significantly higher in K3 at ZT11 under high R/FR. With myo-inositol being involved in numerous biological processes, including auxin biosynthesis, membrane biogenesis, light and abiotic stress responses[53], its modulation likely impacts several of the morphological responses we observe.

Other nutritional compounds - In addition to amino acids and carbohydrates, our metabolite and proteome analyses identified light intensity- and spectra-induced changes in several other compounds beneficial for human nutrition, with some cultivar and time-of-day specific differences. Specifically, we note an increase in ascorbic acid (vitamin C) with increasing light intensity, particularly in K3 at ZT11. Vitamin C has antioxidant properties[54], and this finding corresponds with the finding of superoxide metabolic processes being enriched amongst up-regulated proteins in K3 at ZT11. In addition, the amount of vitamin C in K3 in our R/FR experiments appeared to decrease under the balanced light condition, but increase with an increase in R/FR, indicative of the balanced light condition having the lowest oxidative stress. Conversely, in K9, ascorbic acid increased with increasing R/FR, suggesting different responses to oxidative stress among cultivars, and potentially resulting in increased anthocyanin within K9. It is possible that K3 deals with oxidative stress by increasing ascorbic acid and K9 by

increasing anthocyanin content. The K3 ascorbic acid content is consistent with previous findings of red and far-red light both inducing increases in ascorbic acid content in green pepper fruit[55].

In addition to ascorbic acid, anthocyanins are a natural source of antioxidants, beneficial for human health[56,57], with the generation of anthocyanins typically driven by light[58]. In our study, we were only able to detect anthocyanins within the K9 cultivar, with no significant difference under the changing light intensity conditions applied, but a significant decrease with increasing R/B, and a significant increase with increasing R/FR. Within our metabolite analysis, we observe changes associated with anthocyanin and phenylpropanoid metabolism: including chlorogenic acid and quininic acid with changing R/B, and sinapinic acid, chlorogenic acid, quininic acid and 3-coumaroyl-D-quinic acid changing in R/FR.

Additionally, within our metabolic pathway analysis, we observed significant pathway enrichment associated with phenylpropanoid and flavonoid metabolism with increasing R/B and R/FR composition. Correspondingly, we also see a significant up-regulation of flavonoid biosynthetic pathways, which is more pronounced in the K9 cultivar and consistent with our ability to detect anthocyanins in this cultivar. Intriguingly, we find an up-regulation of phenylpropanoid biosynthesis pathways in K9 with increasing R/B at ZT23, which contrasts our observed anthocyanin levels. It is possible that at ZT23 the phenylpropanoid pathway is diverting the flux toward other phenylpropanoid products. For example, we see the coumarin biosynthesis pathway enriched in our metabolic pathway analysis, coupled with observed up-regulation of DEFECTIVE IN CUTICULAR RIDGES (DCR; A0A0D3DD85), ENHACED PSEUDOMONAS SUSCEPTIBILITY1 (EPS1; A0A0D3D884) and COUMARIN SYNTHASE (COSY; A0A0D3CEC8) in K9 at ZT23, indicating possible increased coumarin biosynthesis[59–61]. Thus, our results suggest the ideal conditions for kale anthocyanin production under lower intensities involves the use of a high R/FR spectral composition, with higher R/B ratios having negative impacts by possibly diverting the phenylpropanoid pathway toward other products. This has substantial application potential for low energy indoor farming.

Although not measured in our metabolomics analysis, our proteomic analysis identified changes in abundance of proteins involved in production of glucosinolates and carotenoids. Individual glucosinolates are typically detected using HPLC, not GC-MS[62,63]. Playing a role in kale flavour and plant defense, glucosinolates can also act as anti-oncogenic compounds for enhanced human health[64]. Our proteomic analyses indicated changes in glucosinolate metabolism with increasing light intensity and R/B ratio. In our intensity experiments, the K9 cultivar showed a down-regulation of proteins associated with glucosinolate catabolism as light

intensity increased. Our metabolic pathway analysis also indicated increased biosynthesis of glucosinolates in K3, thus the cultivars might achieve the same elevated levels of glucosinolates at higher light intensities through differing mechanisms. In our bioinformatics assessment of R/B responses, we find glucosinolate catabolism to be decreased and glucosinolate biosynthesis increased in K3. This has previously been observed with levels of the glucosinolates sinigrin, glucobrassicin, and 4-methoxy glucobrassicin in *B. napus* sprouts exposed to increasing red light levels[65], while another study found differential cultivar responses with changing light intensities in Chinese cabbage[66].

In addition to flavonoids and glucosinolates, carotenoids are also antioxidant compounds beneficial to human health[67]. Within our proteomic data, we find K3 has lower carotenoid production with increasing light intensity, combined with decreasing protein abundance of CAROTENE CIS-TRANS-ISOMERASE (CRTISO; A0A0D3DYP6), 15-CIS-PHYTOENE DESATURASE (PDS; A0A0D3BJ64) and PHYTOENE SYNTHASE1 (PSY1; A0A0D3AJG7). In our spectral experiments, it appears that increasing red light in both the R/B and R/FR experiments drives increased carotenoid biosynthesis in the K9 cultivar, along with increasing protein abundance of CRTISO (A0A0D3DYP6), LYCOPENE EPSILON CYCLASE2 (LUT2; A0A0D3B320), PSY1 and PDS in R/B experiments and PDS, CRTISO and CYP97B3 under R/FR conditions. These results suggest that K3 might be more sensitive to light intensity changes and K9 to levels of red light. We thought it interesting to find lower carotenoid biosynthesis with increasing light intensity in K3 as carotenoids tend to increase with higher light intensity[68], however there is evidence in pepper of lower carotenoids with increasing light intensity that is suggested to be due to a higher photo-oxidation rate than that of carotenoid synthesis[69,70].

Conclusions

We present an integrated, systems-level analysis of two phylogenetically related kale cultivars under increasing light intensity, R/B and R/FR spectral ratios with time-of-day precision. Our dataset reveals that light intensity and spectral composition can modulate myriad processes within kale, eliciting changes in growth, and photosynthetic parameters, as well as cell wall and hormones related to shade avoidance (**Figure 8**). Further, we identify changes in nutritional content such as amino acids, carbohydrates, glucosinolates, and anthocyanins with subtle differences between the K3 and K9 cultivar (**Figure 8**). Collectively, these results provide wide-ranging knowledge to indoor farmers of what genetics offer precise nutritional benefits when

grown under certain conditions. This offers substantial value to indoor farming operations looking to grow diverse leafy greens of enhanced nutritional value.

REFERENCES

1. Satheesh, N. & Workneh Fanta, S. Kale: Review on nutritional composition, bio-active compounds, anti-nutritional factors, health beneficial properties and value-added products. *Cogent Food Agric.* **6**, 1811048 (2020).
2. Rachwał, K. *et al.* Red Kale (Brassica oleracea L. ssp. acephala L. var. sabellica) Induces Apoptosis in Human Colorectal Cancer Cells In Vitro. *Molecules* **28**, 6938 (2023).
3. Bowen-Forbes, C. *et al.* Broccoli, Kale, and Radish Sprouts: Key Phytochemical Constituents and DPPH Free Radical Scavenging Activity. *Molecules* **28**, 4266 (2023).
4. Cao, D. *et al.* Spermidine enhances chilling tolerance of kale seeds by modulating ROS and phytohormone metabolism. *PLOS ONE* **18**, e0289563 (2023).
5. Bauer, N. *et al.* Mechanisms of Kale (Brassica oleracea var. acephala) Tolerance to Individual and Combined Stresses of Drought and Elevated Temperature. *Int. J. Mol. Sci.* **23**, 11494 (2022).
6. Fussy, A. & Papenbrock, J. An Overview of Soil and Soilless Cultivation Techniques—Chances, Challenges and the Neglected Question of Sustainability. *Plants* **11**, 1153 (2022).
7. https://www.alliedmarketresearch.com, A. M. R. Kale Microgreen Market Size, Share, Price, Trends |Research Report 2030. *Allied Market Research* https://www.alliedmarketresearch.com/kale-microgreen-market-A16137.
8. Hati, A. J. & Singh, R. R. Smart Indoor Farms: Leveraging Technological Advancements to Power a Sustainable Agricultural Revolution. *AgriEngineering* **3**, 728–767 (2021).
9. Nájera, C., Gallegos-Cedillo, V. M., Ros, M. & Pascual, J. A. LED Lighting in Vertical Farming Systems Enhances Bioactive Compounds and Productivity of Vegetables Crops. *Biol. Life Sci. Forum* **16**, 24 (2022).

592 10. McCree, K. J. The action spectrum, absorptance and quantum yield of photosynthesis in crop plants.
593 *Agric. Meteorol.* **9**, 191–216 (1971).
594 11. Krahmer, J., Ganpudi, A., Abbas, A., Romanowski, A. & Halliday, K. J. Phytochrome, Carbon Sensing,
595 Metabolism, and Plant Growth Plasticity. *Plant Physiol.* **176**, 1039–1048 (2018).
596 12. Chen, J. *et al.* Effect of Photoperiod on Chinese Kale (Brassica alboglabra) Sprouts Under White or
597 Combined Red and Blue Light. *Front. Plant Sci.* **11**, (2021).
598 13. Kong, Y., Schiestel, K. & Zheng, Y. Pure blue light effects on growth and morphology are slightly
599 changed by adding low-level UVA or far-red light: A comparison with red light in four microgreen
600 species. *Environ. Exp. Bot.* **157**, 58–68 (2019).
601 14. Deng, M. *et al.* Influence of pre-harvest red light irradiation on main phytochemicals and antioxidant
602 activity of Chinese kale sprouts. *Food Chem.* **222**, 1–5 (2017).
603 15. Zhen, S. & van Iersel, M. W. Far-red light is needed for efficient photochemistry and photosynthesis.
604 *J. Plant Physiol.* **209**, 115–122 (2017).
605 16. Furuya, M. & Schäfer, E. Photoperception and signalling of induction reactions by different
606 phytochromes. *Trends Plant Sci.* **1**, 301–307 (1996).
607 17. Scandola, S., Mehta, D., Castillo, B., Boyce, N. & Uhrig, R. G. Systems-level proteomics and
608 metabolomics reveals the diel molecular landscape of diverse kale cultivars. *Front. Plant Sci.* **14**,
609 (2023).
610 18. Kuhlgert, S. *et al.* MultispeQ Beta: a tool for large-scale plant phenotyping connected to the open
611 PhotosynQ network. *R. Soc. Open Sci.* **3**, 160592 (2016).
612 19. Gehan, M. A. *et al.* PlantCV v2: Image analysis software for high-throughput plant phenotyping.
613 *PeerJ* **5**, e4088 (2017).

614 20. Mehta, D., Scandola, S. & Uhrig, R. G. BoxCar and Library-Free Data-Independent Acquisition
615 Substantially Improve the Depth, Range, and Completeness of Label-Free Quantitative Proteomics.
616 *Anal. Chem.* **94**, 793–802 (2022).
617 21. Balázs, L. *et al.* Quantifying the Effect of Light Intensity Uniformity on the Crop Yield by Pea
618 Microgreens Growth Experiments. *Horticulturae* **9**, 1187 (2023).
619 22. Jones-Baumgardt, C., Llewellyn, D., Ying, Q. & Zheng, Y. Intensity of Sole-source Light-emitting
620 Diodes Affects Growth, Yield, and Quality of Brassicaceae Microgreens. (2019)
621 doi:10.21273/HORTSCI13788-18.
622 23. Dou, H. *et al.* Supplementary Far-Red Light for Photosynthetic Active Radiation Differentially
623 Influences the Photochemical Efficiency and Biomass Accumulation in Greenhouse-Grown Lettuce.
624 *Plants* **13**, 2169 (2024).
625 24. Gudžinskaitė, I., Laužikė, K., Pukalskas, A. & Samuolienė, G. The Effect of Light Intensity during
626 Cultivation and Postharvest Storage on Mustard and Kale Microgreen Quality. *Antioxidants* **13**, 1075
627 (2024).
628 25. Boucher, L., Nguyen, T.-T.-A., Brégard, A., Pepin, S. & Dorais, M. Optimizing Light Use Efficiency and
629 Quality of Indoor Organically Grown Leafy Greens by Using Different Lighting Strategies. *Agronomy*
630 **13**, 2582 (2023).
631 26. Zhang, Y., Butelli, E. & Martin, C. Engineering anthocyanin biosynthesis in plants. *Curr. Opin. Plant*
632 *Biol.* **19**, 81–90 (2014).
633 27. Kaur, S. *et al.* Protective and defensive role of anthocyanins under plant abiotic and biotic stresses:
634 An emerging application in sustainable agriculture. *J. Biotechnol.* **361**, 12–29 (2023).
635 28. Dou, H., Niu, G. & Gu, M. Photosynthesis, Morphology, Yield, and Phytochemical Accumulation in
636 Basil Plants Influenced by Substituting Green Light for Partial Red and/or Blue Light. (2019)
637 doi:10.21273/HORTSCI14282-19.

638 29. Anum, H., Cheng, R. & Tong, Y. Improving plant growth, anthocyanin production and oxidative
639 status of red lettuce (*Lactuca sativa* cv. Lolla Rossa) by optimizing red to blue light ratio with a
640 constant green light fraction in a plant factory. *Sci. Hortic.* **338**, 113832 (2024).
641 30. Frąszczak, B. *et al.* Morphological and Photosynthetic Parameters of Green and Red Kale
642 Microgreens Cultivated under Different Light Spectra. *Plants* **12**, 3800 (2023).
643 31. Fu, W., Li, P. & Wu, Y. Effects of different light intensities on chlorophyll fluorescence characteristics
644 and yield in lettuce. *Sci. Hortic.* **135**, 45–51 (2012).
645 32. Miao, Y., Wang, X., Gao, L., Chen, Q. & Qu, M. Blue light is more essential than red light for
646 maintaining the activities of photosystem II and I and photosynthetic electron transport capacity in
647 cucumber leaves. *J. Integr. Agric.* **15**, 87–100 (2016).
648 33. Pierik, R. & de Wit, M. Shade avoidance: phytochrome signalling and other aboveground neighbour
649 detection cues. *J. Exp. Bot.* **65**, 2815–2824 (2014).
650 34. Lv, M. & Li, J. Molecular Mechanisms of Brassinosteroid-Mediated Responses to Changing
651 Environments in Arabidopsis. *Int. J. Mol. Sci.* **21**, 2737 (2020).
652 35. Keuskamp, D. H. *et al.* Blue-light-mediated shade avoidance requires combined auxin and
653 brassinosteroid action in Arabidopsis seedlings. *Plant J.* **67**, 208–217 (2011).
654 36. Klahre, U. *et al.* The Arabidopsis DIMINUTO/DWARF1 Gene Encodes a Protein Involved in Steroid
655 Synthesis. *Plant Cell* **10**, 1677–1690 (1998).
656 37. Ma, L. & Li, G. Auxin-Dependent Cell Elongation During the Shade Avoidance Response. *Front. Plant*
657 *Sci.* **10**, (2019).
658 38. Sasidharan, R. *et al.* Light Quality-Mediated Petiole Elongation in Arabidopsis during Shade
659 Avoidance Involves Cell Wall Modification by Xyloglucan Endotransglucosylase/Hydrolases. *Plant*
660 *Physiol.* **154**, 978–990 (2010).

661 39. Teramoto, H., Nakamori, A., Minagawa, J. & Ono, T. Light-Intensity-Dependent Expression of Lhc
662 Gene Family Encoding Light-Harvesting Chlorophyll-a/b Proteins of Photosystem II in
663 Chlamydomonas reinhardtii. *Plant Physiol.* **130**, 325–333 (2002).
664 40. Anderson, J. M., Chow, W. S. & Goodchild, D. J. Thylakoid Membrane Organisation in Sun/Shade
665 Acclimation. *Funct. Plant Biol.* **15**, 11–26 (1988).
666 41. Anderson, J. M., Chow, W. S. & Park, Y.-I. The grand design of photosynthesis: Acclimation of the
667 photosynthetic apparatus to environmental cues. *Photosynth. Res.* **46**, 129–139 (1995).
668 42. Jin, D. *et al.* Effect of Red and Blue Light on Cucumber Seedlings Grown in a Plant Factory.
669 *Horticulturae* **9**, 124 (2023).
670 43. Lisiewska, Z., Kmiecik, W. & Korus, A. The amino acid composition of kale (*Brassica oleracea* L. var.
671 *acephala*), fresh and after culinary and technological processing. *Food Chem.* **108**, 642–648 (2008).
672 44. Okumoto, S., Funck, D., Trovato, M. & Forlani, G. Editorial: Amino Acids of the Glutamate Family:
673 Functions beyond Primary Metabolism. *Front. Plant Sci.* **7**, (2016).
674 45. Kavi Kishor, P. B. & Sreenivasulu, N. Is proline accumulation per se correlated with stress tolerance
675 or is proline homeostasis a more critical issue? *Plant Cell Environ.* **37**, 300–311 (2014).
676 46. Galili, G. & Amir, R. Fortifying plants with the essential amino acids lysine and methionine to
677 improve nutritional quality. *Plant Biotechnol. J.* **11**, 211–222 (2013).
678 47. Yang, Q., Zhao, D. & Liu, Q. Connections Between Amino Acid Metabolisms in Plants: Lysine as an
679 Example. *Front. Plant Sci.* **11**, (2020).
680 48. Hall, C. J. *et al.* Differential lysine-mediated allosteric regulation of plant dihydrodipicolinate
681 synthase isoforms. *FEBS J.* **288**, 4973–4986 (2021).
682 49. Van Bochaute, P., Novoa, A., Ballet, S., Rognes, S. E. & Angenon, G. Regulatory mechanisms after
683 short- and long-term perturbed lysine biosynthesis in the aspartate pathway: the need for isogenes
684 in Arabidopsis thaliana. *Physiol. Plant.* **149**, 449–460 (2013).

685 50. Rosa-Téllez, S. *et al.* The serine–glycine–one-carbon metabolic network orchestrates changes in
686 nitrogen and sulfur metabolism and shapes plant development. *Plant Cell* **36**, 404–426 (2024).
687 51. Hwang, G. *et al.* Trehalose-6-phosphate signaling regulates thermoresponsive hypocotyl growth in
688 Arabidopsis thaliana. *EMBO Rep.* **20**, e47828 (2019).
689 52. Avidan, O. *et al.* Direct and indirect responses of the Arabidopsis transcriptome to an induced
690 increase in trehalose 6-phosphate. *Plant Physiol.* **196**, 409–431 (2024).
691 53. Sharma, N., Chaudhary, C. & Khurana, P. Role of myo-inositol during skotomorphogenesis in
692 Arabidopsis. *Sci. Rep.* **10**, 17329 (2020).
693 54. Gęgotek, A. & Skrzydlewska, E. Antioxidative and Anti-Inflammatory Activity of Ascorbic Acid.
694 *Antioxidants* **11**, 1993 (2022).
695 55. Pashkovskiy, P. *et al.* Post-Harvest Red- and Far-Red-Light Irradiation and Low Temperature Induce
696 the Accumulation of Carotenoids, Capsaicinoids, and Ascorbic Acid in Capsicum annuum L. Green
697 Pepper Fruit. *Foods* **12**, 1715 (2023).
698 56. Tena, N., Martín, J. & Asuero, A. G. State of the Art of Anthocyanins: Antioxidant Activity, Sources,
699 Bioavailability, and Therapeutic Effect in Human Health. *Antioxidants* **9**, 451 (2020).
700 57. Pojer, E., Mattivi, F., Johnson, D. & Stockley, C. S. The Case for Anthocyanin Consumption to
701 Promote Human Health: A Review. *Compr. Rev. Food Sci. Food Saf.* **12**, 483–508 (2013).
702 58. Liu, C., Yao, X., Li, G., Huang, L. & Xie, Z. Transcriptomic profiling of purple broccoli reveals light-
703 induced anthocyanin biosynthetic signaling and structural genes. *PeerJ* **8**, e8870 (2020).
704 59. Kim, C. Y. *et al.* Emergence of a proton exchange-based isomerization and lactonization mechanism
705 in the plant coumarin synthase COSY. *Nat. Commun.* **14**, 597 (2023).
706 60. Vanholme, R. *et al.* COSY catalyses trans–cis isomerization and lactonization in the biosynthesis of
707 coumarins. *Nat. Plants* **5**, 1066–1075 (2019).

708 61. Rani, S. H., Krishna, T. H. A., Saha, S., Negi, A. S. & Rajasekharan, R. Defective in Cuticular Ridges
709 (*DCR*) of *Arabidopsis thaliana*, a Gene Associated with Surface Cutin Formation, Encodes a Soluble
710 Diacylglycerol Acyltransferase*. *J. Biol. Chem.* **285**, 38337–38347 (2010).
711 62. Grosser, K. & van Dam, N. M. A Straightforward Method for Glucosinolate Extraction and Analysis
712 with High-pressure Liquid Chromatography (HPLC). *J. Vis. Exp. JoVE* 55425 (2017)
713 doi:10.3791/55425.
714 63. Theunis, M. *et al.* Optimization and validation of analytical RP-HPLC methods for the quantification
715 of glucosinolates and isothiocyanates in *Nasturtium officinale* R. Br and *Brassica oleracea*. *LWT* **165**,
716 113668 (2022).
717 64. Ltd, wflpublisher. Comparative study on functional components, antioxidant activity and color
718 parameters of selected colored leafy vegetables as affected by photoperiods. *wflpublisher.com*
719 https://www.wflpublisher.com/Abstract/2605.
720 65. Park, C. H. *et al.* Effects of Light-Emitting Diodes on the Accumulation of Glucosinolates and Phenolic
721 Compounds in Sprouting Canola (Brassica napus L.). *Foods* **8**, 76 (2019).
722 66. Zhou, B. *et al.* Effects of light intensity on the biosynthesis of glucosinolate in Chinese cabbage
723 plantlets. *Sci. Hortic.* **316**, 112036 (2023).
724 67. Eggersdorfer, M. & Wyss, A. Carotenoids in human nutrition and health. *Arch. Biochem. Biophys.*
725 **652**, 18–26 (2018).
726 68. Flores, M., Hernández-Adasme, C., Guevara, M. J. & Escalona, V. H. Effect of different light
727 intensities on agronomic characteristics and antioxidant compounds of Brassicaceae microgreens in
728 a vertical farm system. *Front. Sustain. Food Syst.* **8**, (2024).
729 69. Simkin, A. J., Zhu, C., Kuntz, M. & Sandmann, G. Light-dark regulation of carotenoid biosynthesis in
730 pepper (*Capsicum annuum*) leaves. *J. Plant Physiol.* **160**, 439–443 (2003).

731 70. Pizarro, L. & Stange, C. Light-dependent regulation of carotenoid biosynthesis in plants. *Cienc. E*

732 *Investig. Agrar.* **36**, 143–162 (2009).

733

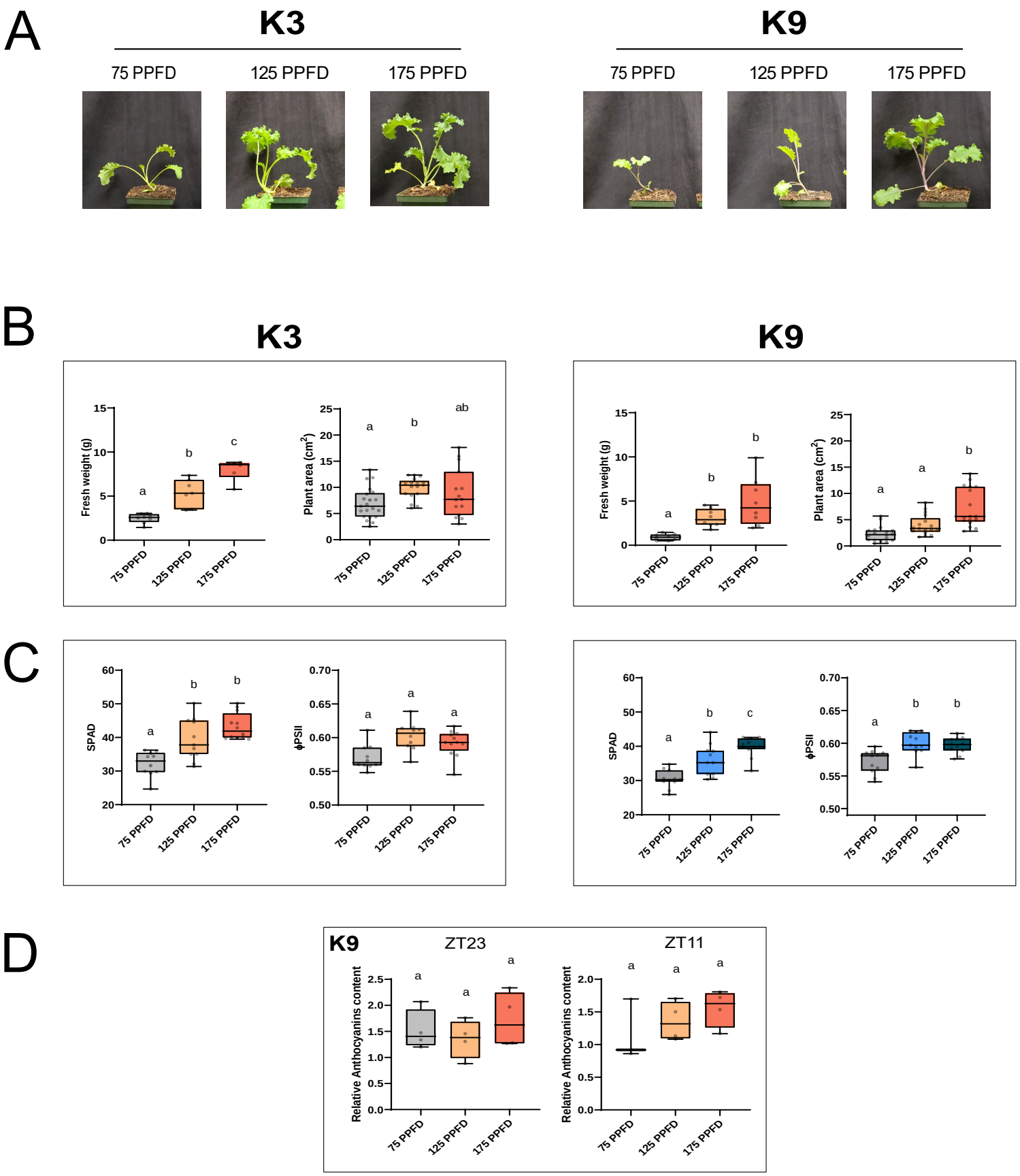

Figure 1. Effect of light intensities on kale growth and development.
A. Pictures of K3 and K9 plants at 35 dpi grown under different light intensities (75, 125, and 175 PPFD).
B. K3 and K9 weight at 35 dpi (n=6), leaf area at 22 dpi (n=15).
C. Relative chlorophyll content (SPAD) and photosynthetic parameters (Phi2) measured with MultispeQ at 35 dpi (n=10).
D. K9 anthocyanin content at 35 dpi (n=4), at different light intensities (75, 125, and 175 PPFD).
Letters shows significant differences using a one-way ANOVA and Tukey's post-hoc test (adjusted p-value <0.05).

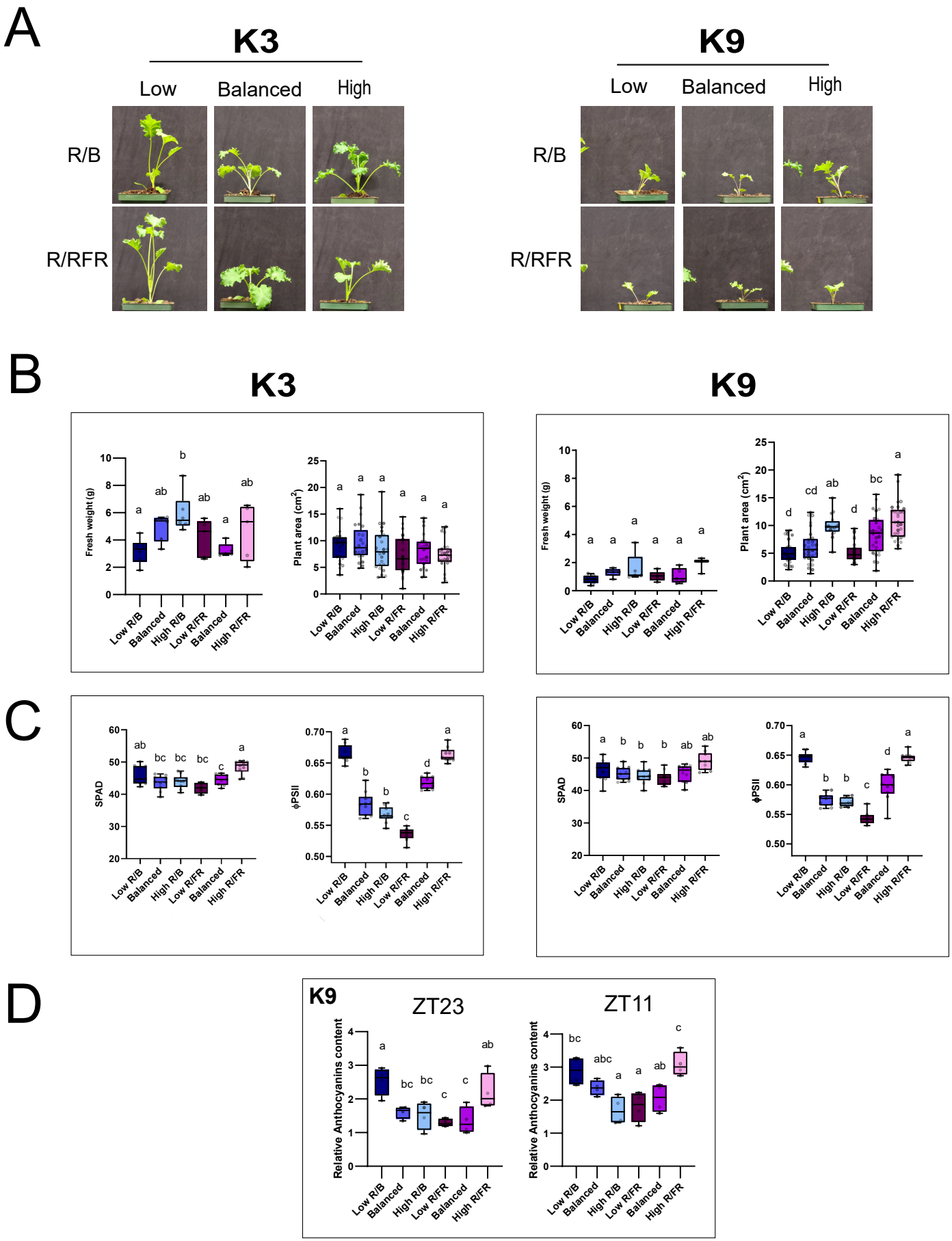

Figure 2. Effect of light spectra on kale growth and development.
A. Pictures of K3 and K9 plants at 35 dpi grown under different light spectra (low, balanced, high R/B and R/FR).
B. K3 and K9 weight at 35 dpi (n=6), leaf area at 22 dpi (n=15), relative chlorophyll content (SPAD) and photosynthetic parameters (Phi2) measured with MultispeQ at 35 dpi (n=10) at different light spectra (low, balanced, high R/B and R/FR).
C. K9 anthocyanin content at 35 dpi (n=4), at different light spectra (low, balanced, high R/B and R/FR).
Letters shows significant differences using a one-way ANOVA and Tukey's post-hoc test (adjusted p-value <0.05).

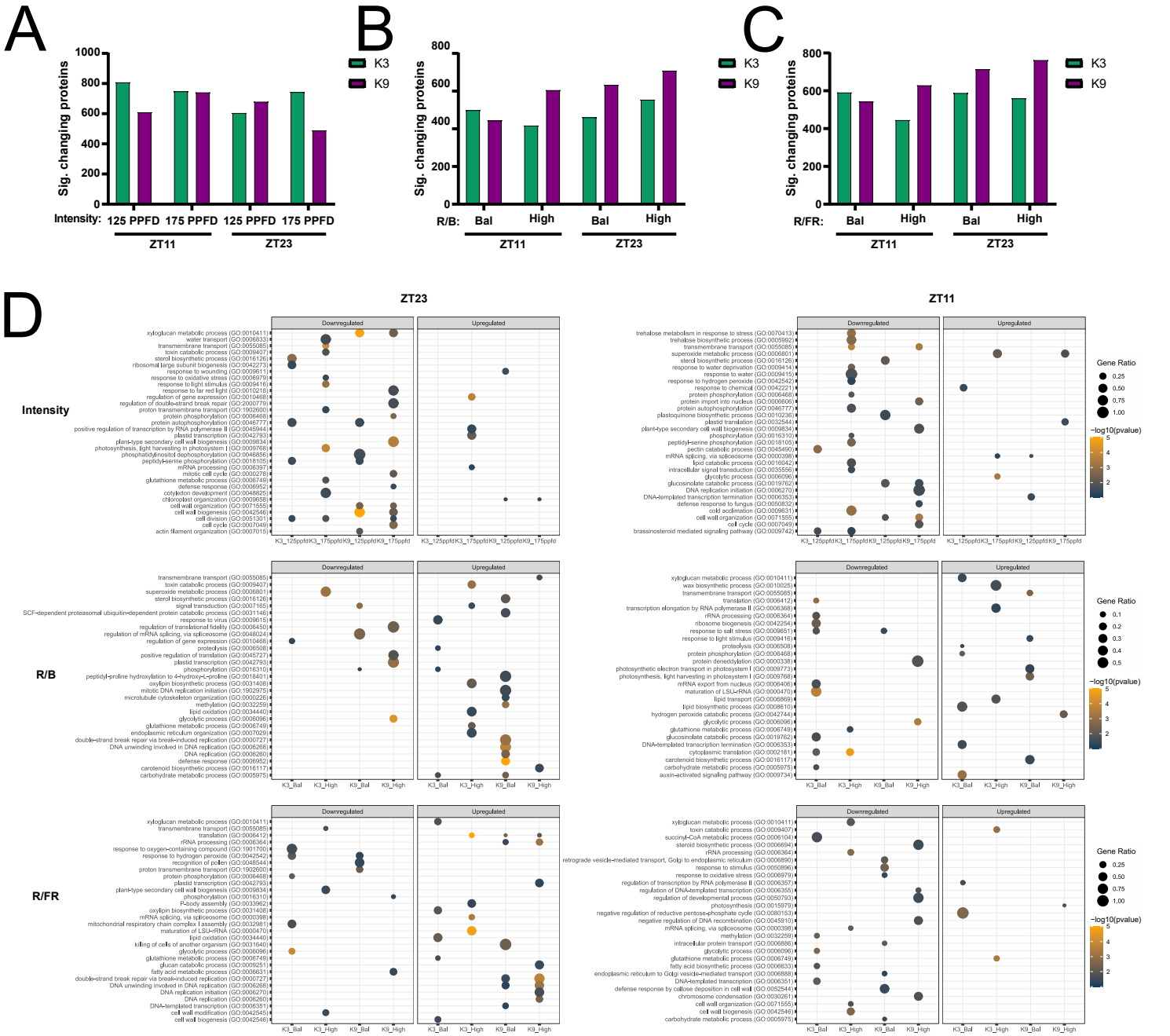

Figure 3. Analysis of significantly changing proteins with changing light intensity and spectral composition.

A-C. Number of proteins with a significant change in abundance with increase in light intensity from 75 PPFD (A), from low R/B (B) and from low R/FR (C).

D. Dot plot representation of enriched GO terms for biological process of significantly changing proteins (q-value < 0.05; Log2FC > 0.58 or < -0.58) that are up- or down-regulated with increasing light intensity (top panel), increasing R/B ratio (middle panel), or increasing R/FR ratio (bottom panel) at ZT23 (left) or ZT11 (right). Dot size indicates the gene ratio (number of proteins in the changing in the condition/total quantified proteins in the category in the study). Dot colour represents the Log10 (p-value). Only GO terms with p-value <0.01 and a total count < 500 are included.

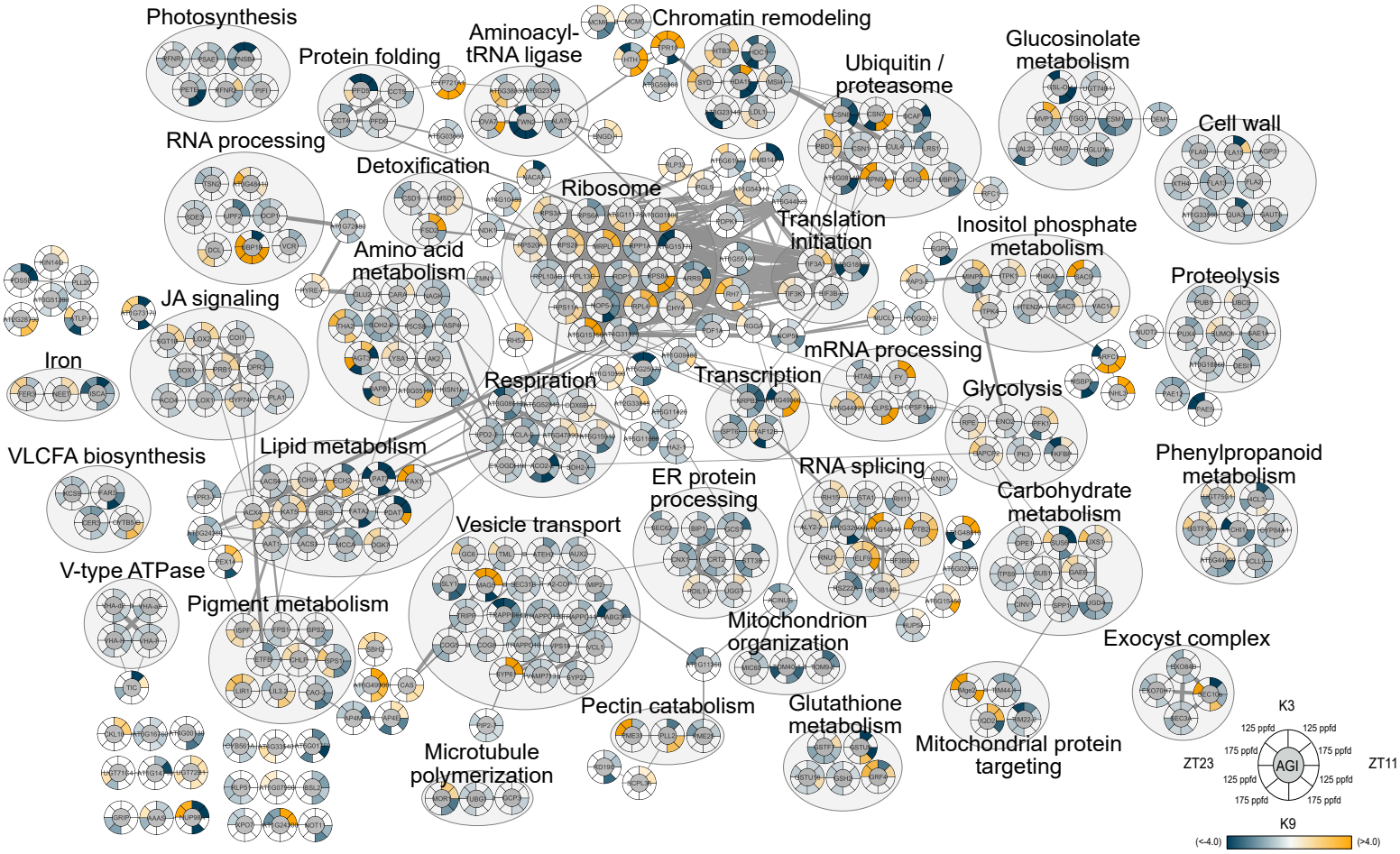

Figure 4. Association network analysis of significantly changing proteins with increasing light intensity
An association network analysis was performed using STRING-DB to depict significantly changing proteins in K3 and K9 kale under increasing light intensity at ZT23 and ZT11. Edge thickness indicates strength of connection between the nodes. Minimum edge threshold was set to 0.95. Protein nodes are labelled either by primary gene name or Arabidopsis gene identifier (AGI). Outer circle surrounding each node represents the standardized relative Log2FC of the indicated significantly changing protein with an increase from 75 PPFD to either 125 PPFD or 175 PPFD in K3 or K9 as indicated by the legend. The scale of blue to yellow indicates the relative decrease or increase in abundance, respectively from 75 PPFD to either 125 PPFD or 175 PPFD. Node groupings are indicated by a grey circle representing proteins involved in the same biological process.

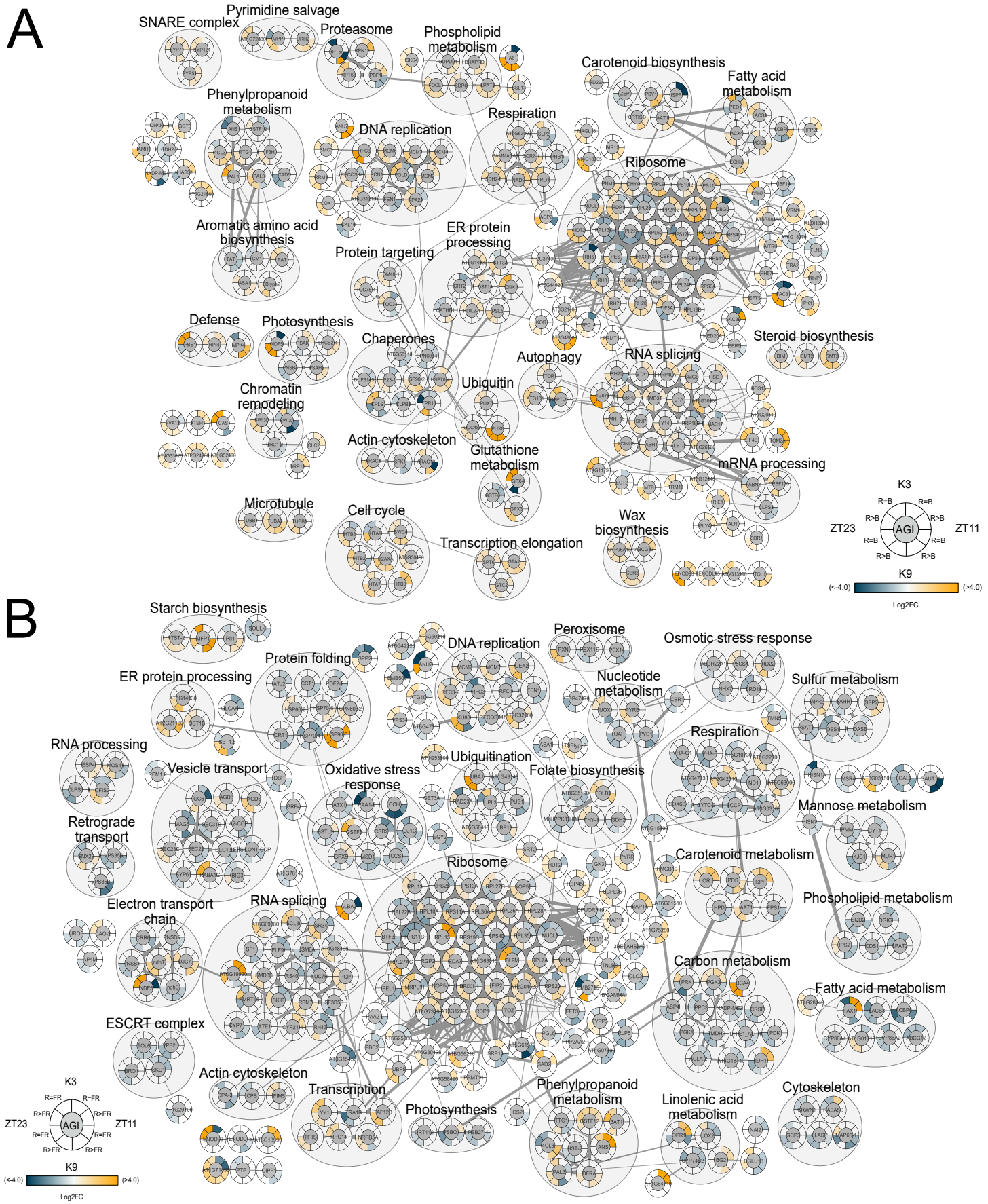

Figure 5. Association network analysis of significantly changing proteins with changing light quality
An association network analysis was performed using STRING-DB to depict significantly changing proteins in K3 and K9 kale under increasing R/B spectral ratio (A) or R/FR ratio (B) at ZT23 and ZT11. Edge thickness indicates the strength of connection between the nodes. Minimum edge threshold was set to 0.95. Protein nodes are labelled either by primary gene name or Arabidopsis gene identifier (AGI). Outer circle surrounding each node represents the standardized relative Log2FC of the indicated significantly changing protein with an increase from low R/B (A) or low R/FR (B) to balanced (R = B) or high R/B (R > B) (A) or balanced (R = FR) or high R/FR (R > FR) (B) in K3 or K9 at ZT23 or ZT11 as indicated by the legend. The scale of blue to yellow indicates the relative decrease or increase in abundance, respectively. Node groupings are indicated by a grey circle representing proteins involved in the same biological process.

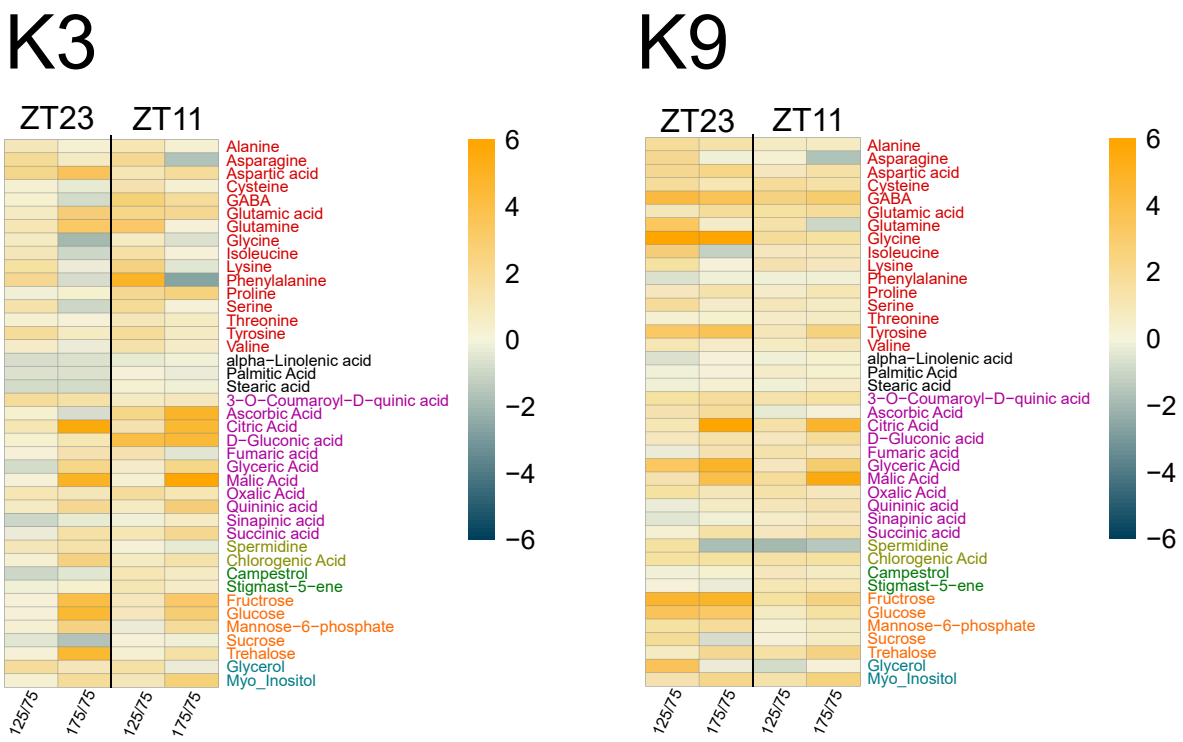

Figure 6: GC-MS analysis of kale cultivars K3 and K9 under different light intensities (75 PPFD, 125 PPFD and 175 PPFD) and at different time of the day (ZT11 and ZT23).
Heatmap of relative cultivars metabolite changes at ZT11 and ZT23 for 125 PPFD/75 PPFD and for 175 PPFD/ 75PPFD. Scale represents log2FC, n=4

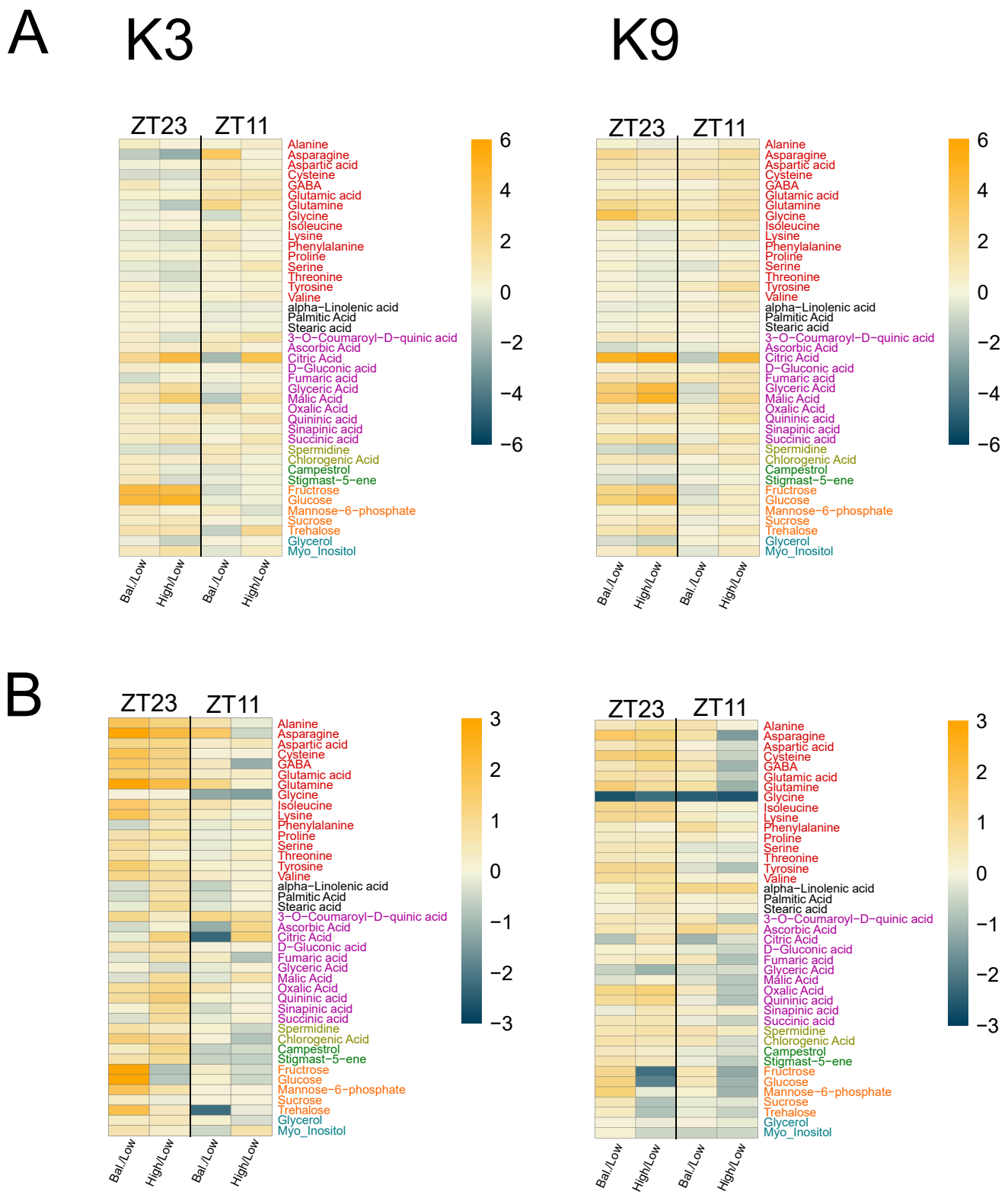

Figure 7: GC-MS analysis of kale cultivars K3 and K9 under different spectral compositions
A) Heatmap of relative cultivars metabolite changes at ZT11 and ZT23 for changing R/B ratio Balanced/Low and High/Low. Scale represents log2FC, n=4
B) Heatmap of relative cultivars metabolite changes at ZT11 and ZT23 for changing R/FR ratio Balanced/Low and High/Low. Scale represents log2FC, n=4

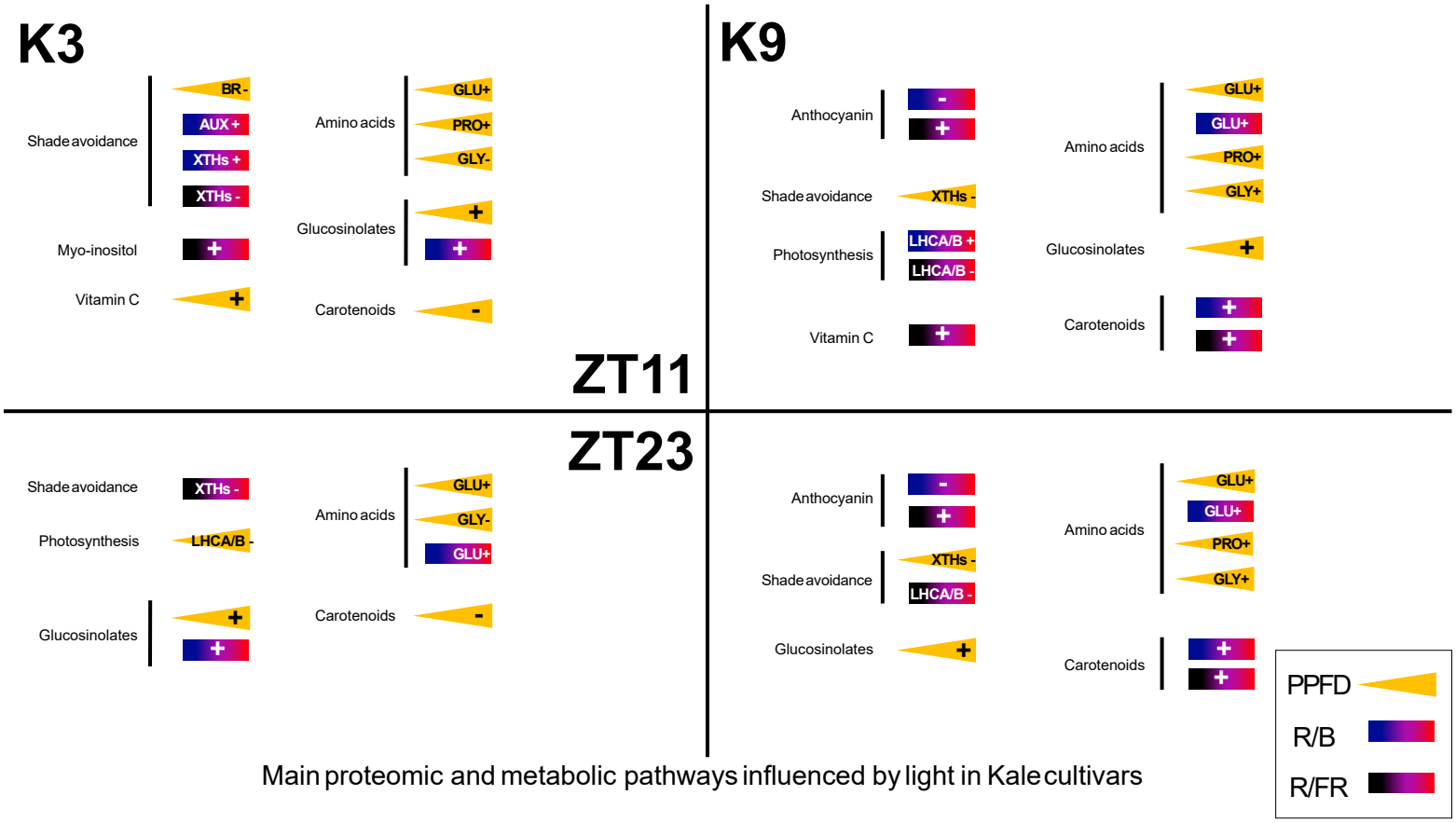

Figure 8. Summary of proteomic and metabolic changes with varying light intensity and spectra
Summary of main proteomic and metabolic pathways influenced by light in kale cultivars K3 and K9 at ZT11 and ZT23 with increasing PPFD, R/B and R/FR.

Table. Effect of light intensity and spectra on photosynthetic parameters measured with the MultispeQ (PhotosynQ Inc.). Relative chlorophyll content (SPAD) and photosynthetic parameters (Phi2, PhiNO, PhiNPQ, LEF, gH^+, ECSt, vH^+) were measured with the MultispeQ at 35 DPI. n=10.

		K3		K9	
	Intensity	**Mean**	**SEM**	**Mean**	**SEM**
SPAD	**75 PPFD**	32.97	3.73	30.24	2.61
	125 PPFD	37.77	6.14	35.22	4.47
	175 PPFD	41.90	3.95	39.93	2.90
Phi2	**75 PPFD**	0.56	0.02	0.58	0.02
	125 PPFD	0.61	0.02	0.60	0.02
	175 PPFD	0.59	0.02	0.60	0.01
PhiNO	**75 PPFD**	0.32	0.02	0.30	0.02
	125 PPFD	0.31	0.03	0.31	0.02
	175 PPFD	0.31	0.01	0.31	0.02
PhiNPQ	**75 PPFD**	0.109	0.015	0.111	0.008
	125 PPFD	0.095	0.022	0.096	0.009
	175 PPFD	0.093	0.019	0.096	0.014
LEF	**75 PPFD**	23.91	2.15	20.37	2.18
	125 PPFD	39.06	4.02	36.72	5.72
	175 PPFD	53.40	9.03	49.33	7.33
gH+	**75 PPFD**	119.61	30.59	115.37	19.10
	125 PPFD	175.33	50.61	110.91	35.23
	175 PPFD	153.41	56.18	117.67	51.88
ECSt	**75 PPFD**	0.008	0.002	0.009	0.002
	125 PPFD	0.006	0.002	0.008	0.003
	175 PPFD	0.007	0.002	0.008	0.006
vH+	**75 PPFD**	0.058	0.013	0.051	0.017
	125 PPFD	0.071	0.018	0.059	0.026
	175 PPFD	0.068	0.023	0.045	0.025

	K3		K9	
R/B	**Mean**	**SEM**	**Mean**	**SEM**
Low	44.70	2.84	47.06	3.23
Balanced	43.80	2.29	45.10	2.09
High	44.14	2.11	44.35	2.47
Low	0.66	0.01	0.65	0.01
Balanced	0.58	0.02	0.58	0.01
High	0.57	0.01	0.57	0.01
Low	0.26	0.01	0.26	0.01
Balanced	0.31	0.02	0.33	0.01
High	0.33	0.02	0.33	0.02
Low	0.086	0.020	0.093	0.009
Balanced	0.089	0.013	0.101	0.006
High	0.112	0.019	0.104	0.017
Low	28.12	1.80	26.60	2.78
Balanced	36.03	4.55	34.02	3.94
High	48.07	6.07	44.81	6.75
Low	147.92	42.54	178.52	50.97
Balanced	170.01	13.77	144.49	42.57
High	162.13	42.77	151.98	47.40
Low	0.007	0.002	0.006	0.002
Balanced	0.006	0.001	0.007	0.002
High	0.006	0.002	0.007	0.002
Low	0.056	0.017	0.062	0.022
Balanced	0.083	0.016	0.069	0.025
High	0.081	0.012	0.082	0.032

	K3		K9	
R/FR	**Mean**	**SEM**	**Mean**	**SEM**
Low	41.98	1.59	44.08	2.14
Balanced	44.57	1.66	46.30	2.70
High	49.09	2.11	48.98	2.71
Low	0.54	0.01	0.54	0.01
Balanced	0.62	0.01	0.60	0.02
High	0.66	0.01	0.65	0.01
Low	0.35	0.02	0.35	0.01
Balanced	0.30	0.02	0.30	0.02
High	0.24	0.01	0.25	0.00
Low	0.110	0.016	0.099	0.014
Balanced	0.086	0.020	0.096	0.010
High	0.097	0.013	0.107	0.014
Low	36.91	1.13	31.47	9.58
Balanced	42.16	4.99	39.07	2.77
High	39.98	1.17	37.25	3.36
Low	152.08	27.80	174.73	56.02
Balanced	173.91	60.05	145.10	52.68
High	150.88	107.37	137.71	48.16
Low	0.007	0.001	0.006	0.002
Balanced	0.006	0.001	0.007	0.002
High	0.007	0.003	0.007	0.002
Low	0.068	0.017	0.066	0.047
Balanced	0.076	0.023	0.075	0.018
High	0.071	0.015	0.072	0.030